

## ARTICLE OPEN



# Vaccination with an HIV T-cell immunogen induces alterations in the mouse gut microbiota

Alessandra Borgognone<sup>1,10</sup>, Aleix Elizalde-Torrent<sup>1,10</sup>, Maria Casadellà<sup>1</sup>, Luis Romero<sup>1,2</sup>, Tuixent Escribà<sup>1</sup>, Mariona Parera<sup>1</sup>, Francesc Català-Moll<sup>1</sup>, Marc Noguera-Julian<sup>1,3,4</sup>, Christian Brander<sup>1,3,4,5,6</sup>, Alex Olvera<sup>1,3,4,11</sup>✉ and Roger Paredes<sup>1,2,3,4,7,8,9,11</sup>✉

The gut microbiota is emerging as a crucial factor modulating vaccine responses; however, few studies have investigated if vaccines, in turn, can alter the microbiota and to what extent such changes may improve vaccine efficacy. To understand the effect of T-cell vaccination on the gut microbiome, we administered an HIV-1 T-cell immunogen (HTI arm) or PBS (control, Mock arm) to C57Bl/6 mice following a heterologous prime-boost scheme. The longitudinal dynamics of the mice gut microbiota was characterized by 16 S ribosomal RNA sequencing in fecal samples collected from cages, as well as from three gut sections (cecum, small and large intestine). Serum and spleen cells were obtained at the last time point of the study to assess immune correlates using IFN $\gamma$  ELISPOT and cytokine Luminex<sup>®</sup> assays. Compared with Mock, HTI-vaccinated mice were enriched in *Clostridiales* genera (*Eubacterium xylanophilum* group, *Roseburia* and *Ruminococcus*) known as primary contributors of anti-inflammatory metabolites, such as short-chain fatty acids. Such shift was observed after the first HTI dose and remained throughout the study follow-up (18 weeks). However, the enriched *Clostridiales* genera were different between feces and gut sections. The abundance of bacteria enriched in vaccinated animals positively correlated with HTI-specific T-cell responses and a set of pro-inflammatory cytokines, such as IL-6. This longitudinal analysis indicates that, in mice, T-cell vaccination may promote an increase in gut bacteria known to produce anti-inflammatory molecules, which in turn correlate with proinflammatory cytokines, suggesting an adaptation of the gut microbial milieu to T-cell-induced systemic inflammation.

npj Biofilms and Microbiomes (2022)8:104; <https://doi.org/10.1038/s41522-022-00368-y>

## INTRODUCTION

It has been well established that the resident gastrointestinal microbiota plays a pivotal role in the development and regulation of both innate and adaptive immune responses<sup>1</sup>. Of the different determinants of the adaptive immune response, T cell response polarization might be especially affected by the gut bacteria composition<sup>2</sup>. In fact, the absence of specific bacteria has been associated with reduced frequencies of Treg cells in the gut<sup>3</sup> or dysregulated Th17 cell responses in germ-free and antibiotic-treated mice<sup>4</sup>. Abnormal ratios of these T cell subpopulations (Th17 and Treg) have been frequently associated with metabolic or immunologic diseases<sup>5</sup>.

Given the tight interaction and co-evolution of gut microbiota and immune system<sup>6</sup>, increasing evidence suggests that certain bacterial taxa might also modulate vaccine-induced immune responses<sup>7</sup>, by exerting local or systemic effects<sup>8</sup>. In recent years, several clinical and animal studies have shown that the composition and functions of the gut microbiota are crucial determinants of the immunogenicity and efficacy of oral and injectable vaccines<sup>9,10</sup>. So far, most work in this area has been focused on the role of the microbiota in modulating vaccine-induced antibody responses<sup>7</sup>. Of note, the importance of T cell-mediated immunity has been increasingly recognized in the protection induced by several immunization strategies, including those against pathogens such as HIV-1<sup>11</sup> or SARS-CoV-2<sup>12</sup>. Yet, a limited number of studies have directly investigated the relationship

between the pre-existing gut microbiota and T cell responses to vaccination<sup>13</sup>.

The effect of vaccine administration on the intestinal microbiota has gathered even less attention. Previous works investigating the effects of HIV-1<sup>14,15</sup> and oral typhoid<sup>16</sup> vaccines on the human gut microbiota reported no discernible perturbations of the microbial community structure induced by vaccination. In contrast, an increase in the *Firmicutes/Bacteroidetes* ratio following HIV-1 DNA/protein immunization was observed in the rectal microbiome of non-human primates<sup>17</sup>. Also, a recent study comparing two SARS-CoV-2 vaccination strategies reported changes in the human gut microbiota 1 month after immunization, characterized by lower alpha diversity and increased abundance of a certain bacterial species, such as *Bacteroides caccae*<sup>18</sup>. Collectively this provides at least circumstantial evidence that vaccination can influence the resident microbiota. Therefore, understanding how vaccines promote changes in the host intestinal immune milieu and alter the microbial community structure, may provide important insight into this interplay and, in turn, the identification of specific bacteria that positively modulate vaccination outcome.

In the present study, HIV-1 T-cell immunogen (HTI) expressing vectors<sup>19,20</sup> were used to assess vaccine-induced changes in the gut microbiota and to identify potential correlates with the immunological response to vaccination in a murine model. The HTI immunogenicity has been tested in both mice<sup>21,22</sup> and humans<sup>23</sup> using different vaccine vectors (such as DNA,

<sup>1</sup>IrsiCaixa AIDS Research Institute, Badalona, Spain. <sup>2</sup>Universitat Autònoma de Barcelona (UAB), Barcelona, Catalonia, Spain. <sup>3</sup>Universitat de Vic-Universitat Central de Catalunya (UVic-UCC), Vic, Spain. <sup>4</sup>Ciber of Infectious Diseases CIBERINFEC, ISCIII, Madrid, Spain. <sup>5</sup>Institució Catalana de Recerca i Estudis Avançats (ICREA), Barcelona, Spain. <sup>6</sup>AELIX Therapeutics, Barcelona, Spain. <sup>7</sup>Center for Global Health and Diseases, Department of Pathology, Case Western Reserve University, Cleveland, OH, USA. <sup>8</sup>Fundació Lluita contra les Infeccions, Hospital Universitari Germans Trias i Pujol, Badalona, Catalonia, Spain. <sup>9</sup>Department of Infectious Diseases, Hospital Universitari Germans Trias i Pujol, Badalona, Catalonia, Spain. <sup>10</sup>These authors contributed equally: Alessandra Borgognone, Aleix Elizalde-Torrent. <sup>11</sup>These authors jointly supervised this work: Alex Olvera, Roger Paredes. ✉email: aolvera@irsicaixa.es; rparedes@irsicaixa.es

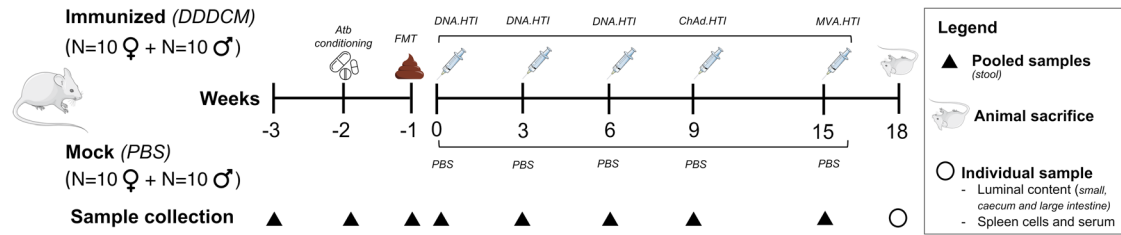


**Fig. 1 Study design and sample collection.** Female and male mice were immunized with an HIV T-cell vaccine (three DNA.HTI primes followed by a ChAd.HTI and MVA.HTI booster;  $n = 20$ ) or a mock vaccine (PBS;  $n = 20$ ). Antibiotic conditioning followed by fecal microbiota transfer was performed prior to vaccination to homogenize the intestinal content across all animals. Collection of samples, including stool, luminal content, serum and spleen was completed at the indicated time points. Abbreviations: FMT fecal microbiota transfer, Atb Antibiotic, PBS phosphate-buffered saline. The Figure was partly generated using Servier Medical Art, provided by Servier, licensed under a Creative Commons Attribution 3.0 unported license.

Chimpanzee Adenovirus, ChAdOx1; Modified Vaccine virus Ankara, MVA and Bacillus Calmette–Guérin, BCG). Based on this previous evidence, mouse strain C57Bl/6 and a three DNA prime followed by a ChAdOx.1—MVA boost were selected to achieve maximal immunogenicity. 16 S rRNA gene sequencing was used to characterize longitudinal fecal microbiome and intestinal content profiles in mice receiving a prime-boost HTI immunization regimen or PBS (control group). Correlations between gut microbial signatures, T cell vaccine response and cytokines after full immunization were also assessed.

## RESULTS

### Study design and sequencing analysis

To investigate the effects of HTI vaccination on the gut microbiota, two experimental groups receiving the HTI immunogen (Immunized,  $n = 20$ ) or PBS (Mock,  $n = 20$ ) were compared (Fig. 1). Fecal samples were collected longitudinally from cages and from three gut sections for gut microbiome profiling; serum and splenocytes were obtained at the end of the study to assess vaccine immunogenicity and cytokine profiles, respectively (Supplementary Fig. 1). Two weeks before vaccination, the mice gut microbiota was homogenized by antibiotic conditioning followed by mouse-to-mouse fecal microbiota transfer (FMT) to reduce baseline variability, as detailed in Supplementary Text and Supplementary Fig. 2. Baseline mouse characteristics at animal arrival (-3w; Supplementary Tables 1 and 2) and pre-vaccination (0w; Table 1 and Supplementary Table 3) are reported.

Mock and Immunized longitudinal samples had no differences in the number of high-quality filtered reads, with a median of 52,092 and 46,584 reads, respectively (Supplementary Fig. 3a and Table S4). Negative extraction ( $n = 12$ ) and no-template PCR ( $n = 11$ ) controls had significantly lower number of reads (5966 and 1444 mean read number, respectively) compared to the experimental groups (Supplementary Fig. 3a). Despite the sequencing depth was higher in batch 1 (Supplementary Fig. 3b), no substantial impact on data structure was observed after assessing for differences between the two batches (Supplementary Fig. 4) (batch was included as a covariate in testing for pooled fecal samples collected from cages).

### Longitudinal assessment of microbiota composition and diversity after HTI vaccination

Prior vaccination, samples displayed similar bacterial composition (0 week, Supplementary Fig. 2) and only the genus A2 was increased in the Mock group (Supplementary Fig. 5a). After segregating by sex, female mice showed higher abundance of *Lactobacillus* and *Muribaculum* before vaccination (Supplementary Fig. 5b).

At family-level, the overall microbial community composition between Mock and Immunized groups was similar over the

experiment (Fig. 2a). Samples from both fecal and luminal content were dominated by *Muribaculaceae* (49.8% and 57.9%), *Lachnospiraceae* (14.2% and 11.4%), *Bacteroidaceae* (9.4% and 4.8%) and *Bifidobacteriaceae* (7.1% and 6.2%) (Fig. 2a and Supplementary Fig. 6a), except for the small intestine (Supplementary Fig. 6b). In this gut section, reduction in *Lachnospiraceae* NK4A136 group (0.2%) and *Bacteroides* (0.05%) was concomitant to an overall increase in *Lactobacillus* (7.7%) and *Ligilactobacillus* (3.7%) (Supplementary Fig. 6c, d). Despite overall compositional similarities during the vaccine administration (0 week–15 week, Fig. 2a and Supplementary Fig. 6e), samples clustered separately by experimental group ( $p = 0.022$ ), but not by timepoint within each group ( $p = 0.594$ ) (Fig. 2b), as indicated by both univariate and multivariate analyses (Supplementary Table 5). Cage and Sex covariates also showed a significant impact on the microbiota composition (Supplementary Table 5). Despite the lack of individual-level contribution in our assessments, a trend toward higher Bray–Curtis dissimilarity in the Immunized compared to the Mock group was observed (Supplementary Fig. 6f), potentially indicating a strong impact on the gut microbiota of vaccinated mice. Also, no differences in alpha diversity (Shannon index) were observed between groups during vaccination (Supplementary Fig. 6g). Clustering by experimental group ( $p = 0.021$ ) and intestinal section ( $p = 0.001$ ) was also observed at the last time point of the study, being samples from small intestine separated from those from caecum and large intestine (Fig. 2c). Moreover, samples from the small intestine showed lower alpha diversity in both Mock and Immunized groups when compared to caecum and large intestine, although no differences between the two experimental groups were detected (Fig. 2d).

### Gut microbiota alterations associated to HTI vaccination

The longitudinal discriminant analysis showed that the abundance of specific bacteria changed after vaccination. While only the A2 genus was differentially abundant between experimental groups at the baseline (Supplementary Fig. 5a), the Immunized group showed an enrichment in a set of *Clostridiales* genera after vaccination (Fig. 3). The most remarkable observation was an enrichment in *Ruminococcus* in fecal samples from cages (week 3–15) and *Roseburia* in gut sections (caecum and large intestine), while *Eubacterium xylanophilum* group remained consistently higher in fecal samples from cages and gut sections after week 3. Also, *Ligilactobacillus* was increased specifically in samples from the small intestine (Fig. 3). Longitudinal assessment of such genera abundance indicated an increasing trend starting at vaccination in the Immunized group (Supplementary Fig. 7). Conversely, no specific genera were consistently higher in the Mock group over time.

**Table 1.** Baseline characteristics at baseline (0 week, pre-vaccination).

Group	Mouse Line	Age (weeks)	Cage	N mice	Sex	Weight (g ± SD)	Sequencing Batch	Microbiota composition <sup>2</sup>
Mock	C57BL/6J01aHsd	9	C19	5	F	19.3 ± 0.9	B1	<i>Lachnospiraceae</i> NK4A136 group (10.8%), <i>Bifidobacterium</i> (5.7%), <i>Bacteroides</i> (5.3%), <i>Lactobacillus</i> (3.4%), <i>Turicibacter</i> (1.7%)
Mock	C57BL/6J01aHsd	9	C20	5	M	25.4 ± 1.4	B1	<i>Bacteroides</i> (11.4%), <i>Lachnospiraceae</i> NK4A136 group (7.9%), <i>Bifidobacterium</i> (6.2%), <i>Alistipes</i> (2.5%), <i>Anaerostipes</i> (1.7%)
Mock	C57BL/6J01aHsd	9	C31	5	F	19.4 ± 1	B2	<i>Bacteroides</i> (16.3%), <i>Lachnospiraceae</i> NK4A136 group (12.2%), <i>Bifidobacterium</i> (5.1%), <i>Lactobacillus</i> (3.1%), <i>Mucispirillum</i> (2.7%)
Mock	C57BL/6J01aHsd	9	C32	5	M	25.3 ± 1.3	B2	<i>Bacteroides</i> (19.2%), <i>Bifidobacterium</i> (10.4%), <i>Lachnospiraceae</i> NK4A136 group (10.1%), <i>Alistipes</i> (3.2%), <i>Lactobacillus</i> (2.1%)
Immunized	C57BL/6J01aHsd	9	C21	5	F	19.5 ± 0.9	B1	<i>Bacteroides</i> (11.7%), <i>Lachnospiraceae</i> NK4A136 group (11.7%), <i>Bifidobacterium</i> (6.6%), <i>Alistipes</i> (1.8%), <i>Lactobacillus</i> (3.9%)
Immunized	C57BL/6J01aHsd	9	C22	5	M	25.6 ± 2	B1	<i>Lachnospiraceae</i> NK4A136 group (14.1%), <i>Bifidobacterium</i> (7.4%), <i>Bacteroides</i> (6.7%), <i>Alistipes</i> (3.2%), <i>Lactobacillus</i> (1.6%)
Immunized	C57BL/6J01aHsd	9	C29	5	F	17.2 ± 0.6	B2	<i>Bacteroides</i> (14.1%), <i>Bifidobacterium</i> (12.9%), <i>Lachnospiraceae</i> NK4A136 group (8.5%), <i>Lactobacillus</i> (3.4%), <i>Faecalibaculum</i> (2.1%)

<sup>1</sup>mean grams and sd.<sup>2</sup>percentage of top 5 most abundant taxa; complete list of taxa is provided in Supplementary Table 3.

### Correlations between gut microbial signatures and immunological responses

To examine the HTI immunogenicity, IFN $\gamma$  assay assessing magnitude and breadth of the specific T cell response against HTI peptides was performed in splenocytes collected at the last time point of the study. No differences in the background IFN $\gamma$ -producing splenocytes were found between Mock and Immunized mice, indicating that the vaccination regimen did not induce noticeable unspecific T cell activation (Supplementary Fig. 8a). After specific re-stimulation with peptide pools covering the HTI sequence, Mock group did not show any IFN $\gamma$  response above the thresholds. In contrast, Immunized mice showed strong responses, in both magnitude (median = 1560 IFN- $\gamma$  SFC/million splenocytes,  $p = 0.00031$ , Supplementary Fig. 8b) and breadth (median = 8.0 out of 17 positive pools,  $p = 0.00028$ , Supplementary Fig. 8c) compared to Mock.

After assessing serum levels of 22 cytokines in Mock and Immunized groups (Supplementary Fig. 9a), IL-6 was the only cytokine showing an increasing trend in the Immunized group after segregating by sex ( $p = 0.052$ ) (Supplementary Fig. 9b), although significance did not pass multiple testing correction (BH-adjusted  $p = 0.69$ ). Specifically, females from the Immunized group showed lower IL-6 levels than males in both Immunized and Mock groups (Supplementary Fig. 9b). We next examined potential links between HTI-specific responses, serum cytokine levels and discriminant bacterial genera. *Eubacterium xylanophilum* group and *Roseburia* from the three intestinal sections were positively correlated with vaccine-induced HTI-specific T cell response (Fig. 4), measured as magnitude and breadth. In addition, most of the tested cytokines showed positive correlations with *Eubacterium xylanophilum* group, *Roseburia* and *Ruminococcus*, although there were some exceptions (i.e., IL-33). An opposite trend was observed for *Ligilactobacillus*, which overall showed negative associations with the serum cytokine levels (Fig. 4). Of note, IL-6 was positively associated with *Eubacterium xylanophilum* group, *Ruminococcus* and especially *Roseburia* in the large intestine. Moreover, *Roseburia* showed positive correlations with other cytokines, including GM-CSF, IL-2, IFN $\gamma$ , IL-17A and IL-25 (small intestine), IL-27 (caecum and large intestine) and IL-22 (large intestine). Significant correlations were confirmed by individual scatterplots (Supplementary Fig. 10). Moreover, *Eubacterium xylanophilum* group, *Roseburia* and *Ruminococcus* from the three intestinal compartments clustered close to the HTI-specific responses (magnitude and breadth) in a hierarchical clustering, also displaying positive associations with a group of cytokines (Supplementary Fig. 11).

### DISCUSSION

To date, limited studies have investigated how vaccine administration may alter resident gut microbial communities. Herein, we used a prime-boost regimen combining the HTI insert in different vaccine vectors, to induce strong HTI-specific responses and study their impact on the microbiota. These results showed, in mice, an increase in *Clostridiales* bacteria following HIV T-cell immunization, which in turn associate with proinflammatory cytokines. Except for *Eubacterium xylanophilum* group, *Clostridiales* genera found in feces were different from those in the three gut sections in the Immunized group. Such differences might be related to the presence of distinct species in the intestinal epithelium compared to the lumen<sup>24</sup> and the presence of a 50-60% spore forming bacteria, like *Ruminococcaceae* and *Lachnospiraceae*, most likely to be present in feces<sup>25</sup>. Remarkably, associations between enriched bacteria and serum cytokines varied across the three intestinal sections, being representative of distinct oxygen requirements and a different crosstalk between mucosal cells and co-existing microbial communities<sup>26</sup>. The most prominent difference was

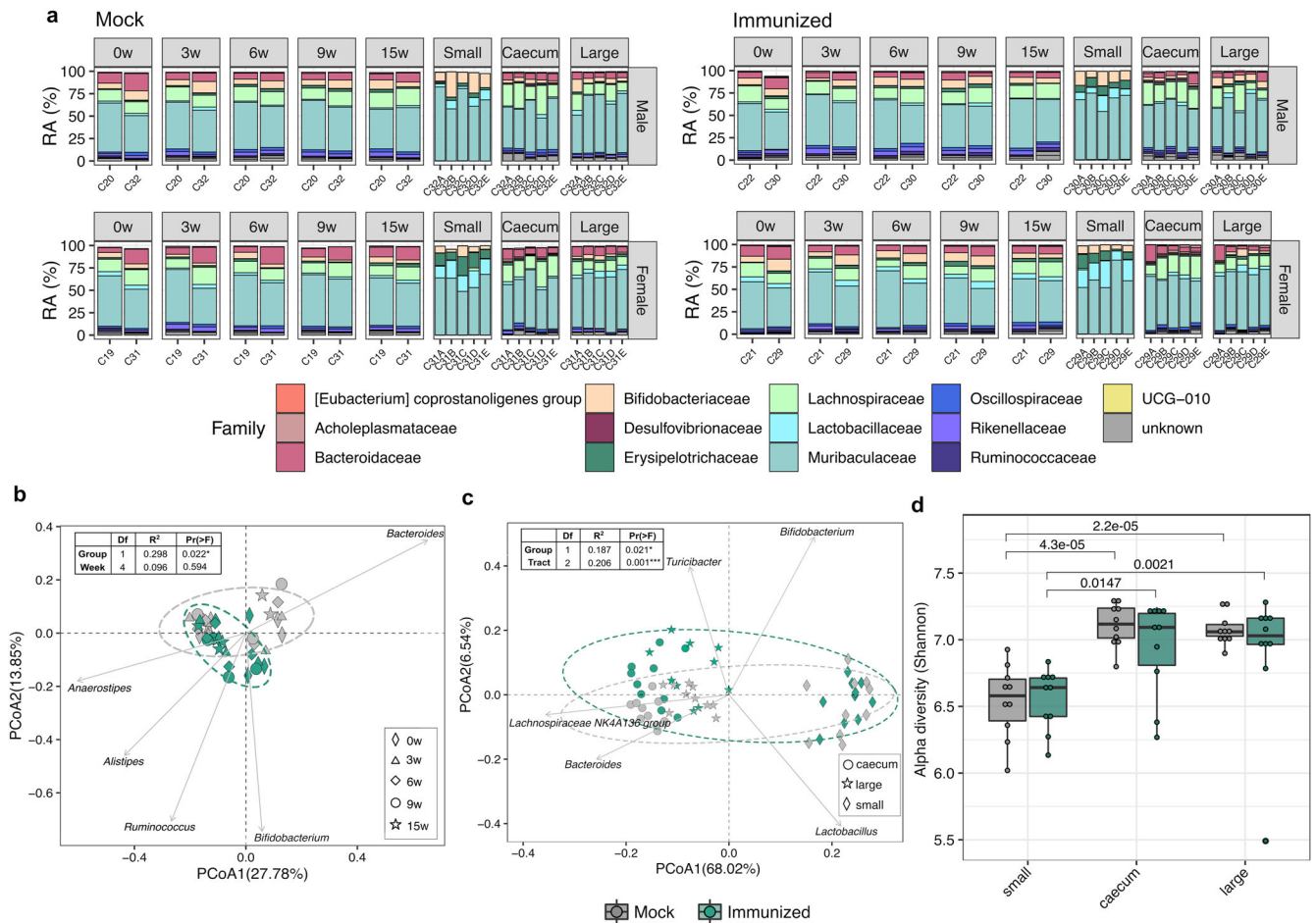


**Fig. 2** Temporal dynamics in microbiome composition after vaccination. **a** Stacked bar chart displaying the relative abundance of bacterial families (top 15 most abundant) at different timepoints in HTI-vaccinated (Immunized) or PBS-vaccinated (Mock) mice. CagelD (pooled feces) and individual samples for each cage (intestinal content) are reported in the x-axis. PCoA biplot based on the first and second components (Bray–Curtis distances at genus level) of **(b)** fecal samples from cages **(c)** and from gut sections (small intestine, caecum and large intestine). Biplots report genera with the top 5 effects on the community composition, with vector position indicating the direction of the effect. Arbitrary ellipses were drawn to facilitate the interpretation of the figure. PERMANOVA r-squared and p-values are shown. **d** Alpha diversity based on Shannon entropy index (ASV level) of individual fecal samples obtained at the last point of the study from small intestine, caecum and large intestine. Boxplots are colored by the experimental group. Median values and interquartile ranges are shown in boxplots. p-values from Wilcoxon signed rank tests are reported.

observed in the small intestine, which was depleted in obligate anaerobes bacteria, such as *Ruminococcaceae* and *Lachnospiraceae*, compared to the caecum and large intestine, as previously reported<sup>27</sup>.

Supporting our results, a recent study in rhesus macaques showed that vaccination with three HIV-1 Env expressing DNA plasmid vaccines followed by a gp140 protein booster induced changes in the rectal microbiota, resulting in increased *Firmicutes/Bacteroidetes* ratio as well as associations of rectal anti-HIV-1 IgG vaccine responses with increased *Clostridium IV* and reduced *Prevotella*<sup>17</sup>. Enrichment in *Ruminococcus* in the intestinal microbiota of piglets was also reported after immunization with *Lawsonia intracellularis* vaccine<sup>28</sup>. In parallel, increased *Bacteroides* abundance along with alterations in the microbial community structure were found following Mtb vaccine (with ESAT6 adjuvanted with TLR8 agonists) administration in mice<sup>29</sup>. Similarly, an enrichment in *Bacteroides caccae* and reduction in clostridial species, such as *Coprococcus comes*, *Dorea longicatena* and *Ruminococcus obeum* were reported in Covid-19 vaccinees<sup>18</sup>. Such apparently conflictive trends indicate that a more thorough understanding is needed to decipher specific microbial shifts induced by distinct immunization strategies.

Our data indicated that bacteria increased after HTI vaccination (*Eubacterium xylanophilum* group, *Roseburia* and *Ruminococcus*), located in the three distinct gut sections, positively correlated with HTI-specific T cell response and a group of serum cytokines. Specifically, the genus *Roseburia*, known as a butyrate-producing bacteria<sup>30</sup>, in the caecum and large intestine, positively correlated with the magnitude and breadth of HTI specific T-cell response in spleen cells. At serum level, *Roseburia* correlated with IL-27, which is produced by antigen presenting cells and regulates B and T cells<sup>31</sup>. Interestingly, despite its different effector function, IL-27 shares the gp130 receptor subunit with IL-6<sup>32</sup> and both cytokines and IL-22 were associated with the content of *Roseburia* in the large intestine. Although the levels of *Roseburia* in small intestine did not correlate with HTI-specific T cell responses, strong correlations were observed with inflammatory cytokines (IL-6, GM-CSF), two Th1 polarization cytokines (IFN $\gamma$  and IL-2) and the Th17 polarization cytokines (IL-17A and IL-22). However, none of these cytokines were differentially produced between the Mock and the Immunized group and only IL-6 showed a marginal significance, which did not pass multiple comparison correction. We hypothesize that the abundance of *Roseburia* may increase due to T cell vaccine stimulation and relate to Th1 responses, as

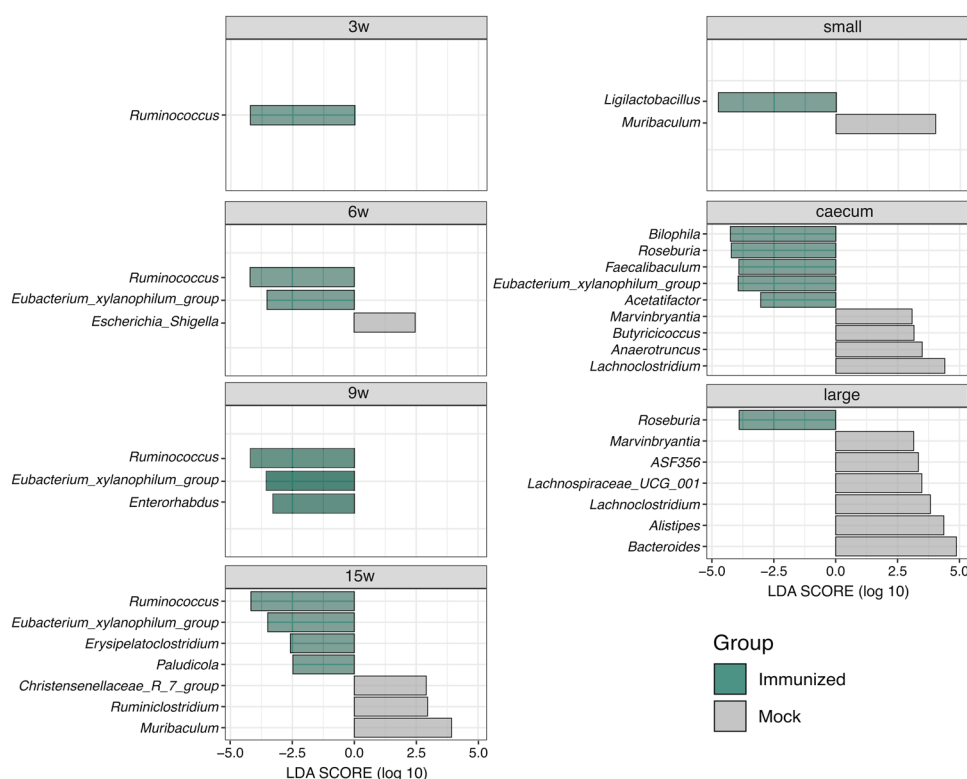


**Fig. 3 Discriminative genera between HTI- and PBS-immunized mice following vaccination.** LEfSe analysis comparing the relative abundance of bacterial genera between Immunized and Mock groups during vaccine administration (pooled fecal samples at 3 week, 9 week, 6 week and 15 week) and at end of study at week 15 for individual fecal samples from small intestine, caecum and large intestine. Horizontal bars represent the effect size for each discriminant genus ( $p < 0.05$  and LDA scores  $> 2.0$ ). The bar length represents the log<sub>10</sub> transformed LDA score, indicated by vertical lines.

indicated by positive correlation with IFN $\gamma$  and IL-2 in plasma, but most remarkably with the HTI-specific T cell responses in spleen cells. The increase in *Roseburia* may be also related to the presence of inflammation mediators such as IL-6<sup>33</sup>, likely produced after vaccination and Th17 (IL-17A and IL-22) cytokines in serum, which could be affecting mucosal immune responses in the gut. Additional butyrate producing *Clostridiales* genera<sup>34</sup> enriched in vaccinated animals showed positive correlations with the HTI-specific T cell responses (*Eubacterium xylanophilum* group in small intestine and caecum) and serum levels of IL-6 (*Ruminococcus* and *Eubacterium xylanophilum* group in large intestine). Also, although *Ligilactobacillus* did not associate with T cell responses, correlations with cytokines representatives of Th17 and Treg population (IL-10 and IL17A), known as gut inflammation biomarkers<sup>35</sup>, might indicate specific changes in the microbiota composition. While the exact mechanism by which HTI-immunization would induce changes in the intestinal milieu and promote an increase of specific bacteria remains unclear, cytokine signaling after innate immunity and T cell activation by vaccination is a plausible hypothesis. In fact, intramuscular vaccine administration may induce local 'depot' effect. This consists in a prolonged antigen release at the site of injection, which induce persistent stimulation of the immune system and recruitment of macrophages that, in turn trigger activation of inflammatory mediators<sup>36</sup>. Of note, administration of viral vaccine vectors rich in Pathogen Associated Molecular Patterns (PAMP), as used in this study, can also trigger the activation of Pathogen Recognition Receptors (PRRs), stimulating the production of pro-inflammatory cytokines, such as IL-1 and TNF- $\alpha$  by dendritic cells and macrophages<sup>37</sup>. Inflammation mediators can then migrate through the bloodstream and lymph vessels to reach intestinal tissues and promote local changes in the immune response and,

in turn, alter the associated microbiota structure<sup>38</sup>. Furthermore, immune cells, such as dendritic cells or regulatory T cells, activated at the site of infection, can mediate inflammatory signaling to the lymph nodes, including mesenteric lymph nodes or the Peyer Patches<sup>39</sup>.

Notably, bacteria correlated with pro-inflammatory cytokines (such as IL-6, IL-27 and IFN $\gamma$ ) in our study (*Roseburia*, *Ruminococcus* and *Eubacterium*) are known as primary contributors of anti-inflammatory metabolites, mainly short chain fatty acids (SCFAs), in the gut<sup>40</sup>. This finding may appear inconsistent with previous evidence, such as in inflammatory bowel diseases, in which SCFAs inhibit the production of pro-inflammatory cytokines<sup>41</sup>; although, several mechanisms by which commensal bacteria can adapt to inflamed gut environment have been discussed elsewhere<sup>42</sup>. For example, specific components of the gut microbiota have been implicated in the production of pleiotropic cytokines by innate immune cells, such as IL-6, and subsequent expansion of Th17 cells<sup>43</sup>, which are critical for vaccine-induced memory immune responses<sup>44</sup>. Also, flagellin and peptidoglycans produced by gut bacteria, such as *Ruminococcus* spp.<sup>45</sup>, can be sensed by pattern recognition receptors (PRRs) expressed by T cells and B cells and act as natural adjuvants to vaccines<sup>7</sup>. In fact, higher abundances of bacteria with flagella and fimbriae, including butyrate-producing such as *Roseburia* and *Eubacterium*, can boost vaccine immunogenicity serving as adjuvants through immunomodulatory TLR agonists<sup>46</sup>.

Notably, members of these bacterial groups, such as *Roseburia intestinalis* and *Eubacterium hallii* have been listed as probiotic candidates by the International Scientific Association for Probiotics and Prebiotics<sup>47</sup>. Indeed, some butyrate-producing bacteria, including those identified in this study, have been shown to modulate the colonic luminal metabolome, regulate T-cell

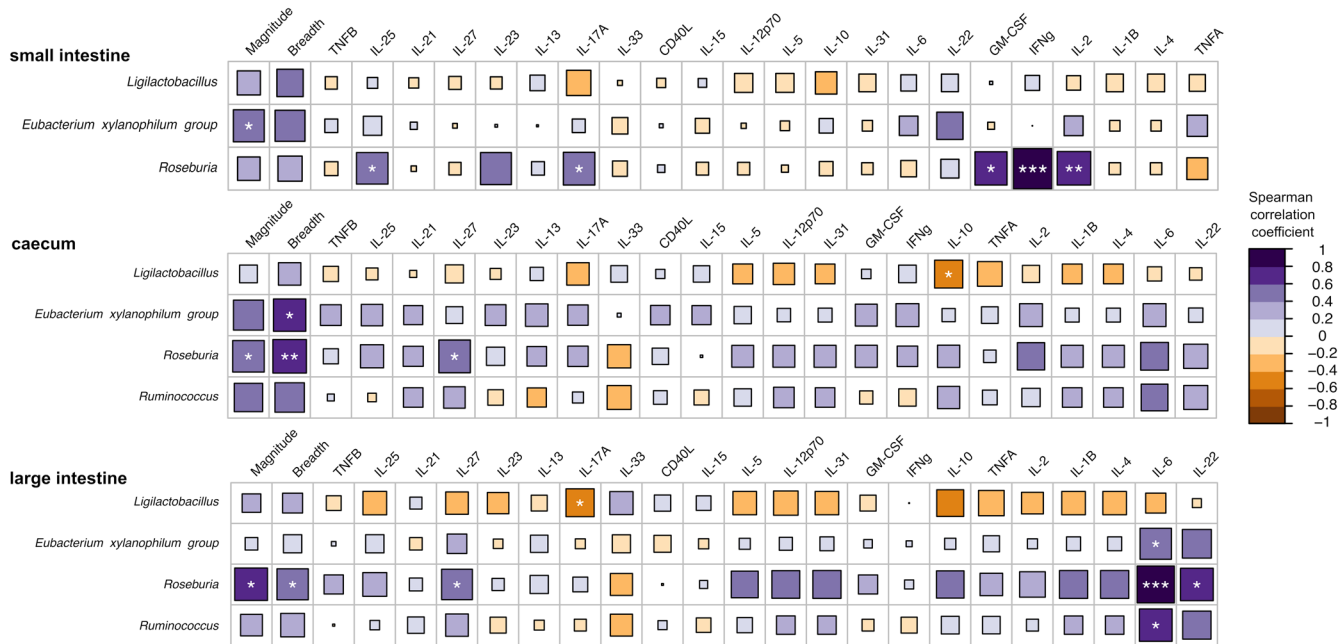


**Fig. 4 Correlation analysis between discriminant bacteria, serum cytokines and immunological responses at the last time point of the study.** Spearman rank correlations between bacterial genera (only bacteria longitudinally enriched in HTI-immunized mice were evaluated), HTI immunogenicity (magnitude and breadth of the response) and serum cytokine levels. Associations are assessed for each gut section (small intestine, caecum and large intestine). Cytokines for each gut section are ordered based on unsupervised hierarchical clustering. Color and size of the square represent the magnitude of the correlation. Significance is indicated by white asterisks (\* $p < 0.05$ ; \*\* $p < 0.01$ ; \*\*\* $p < 0.001$  after Benjamini–Hochberg adjustment for multiple comparisons).

responses and enhance regulatory T-cell functions<sup>48</sup>. Collectively, these data prompted the hypothesis that bacteria producing anti-inflammatory molecules may adapt to increased local inflammation following vaccination, colonize the intestinal milieu and thrive in it, thereby modulating and quenching the inflammatory processes. However, further work is needed to understand how vaccine-induced inflammation promotes an increase of anti-inflammatory bacteria in the gut. In this context, Th17/Treg cell balance, T cell polarization and activation profiles, ILC responses and Kyn/Trp ratio<sup>49</sup> in the gut tissues are promising candidates for future validations. Also, additional omics approaches, including metabolite and targeted SCFA measurements, would help to identify potential anti-inflammatory pathways induced after HTI vaccination. We fully acknowledge the limitation of the small sample size and lack of individual-level contribution in this study. Also, the lack of longitudinal cytokine measurement did not allow us to identify temporal variations of immune correlates with specific bacterial signatures at each stage of the vaccine regimen. Despite a group of bacteria showed strong correlations with HTI-specific T cell responses, another limitation was that the experimental design did not allow to differentiate to which extent vaccine-induced microbiota changes were due to an adjuvant effect of the vectors or to insert-specific responses. Future experiments including a control arm using empty vectors will help to discriminate the direct contribution of the vaccine insert on gut microbiota changes. In addition, another intrinsic limitation was the inability of the 16 S rRNA gene sequencing to distinguish live organisms from transient microorganism colonization<sup>50</sup>. Finally, host-specificity of the core gut microbiota may limit potential extrapolation of these results from a mouse model to humans. Thus, clinical trials including microbiota characterization are needed to validate such findings in the human gut microbiota.

In summary, our data suggest that gut bacteria can adapt to vaccine-induced inflammation. Also, they establish a framework for future studies to fully capture the dynamics of microbial shifts

to T-cell vaccination and, ultimately provide new potential targets for optimizing vaccine efficacy.

## METHODS

### Mice and housing

Six-week-old C57BL/6JOLAHSd mice ( $n = 40$ , 20 females and 20 males), grown in the same breeding facility, were purchased from Envigo and housed under specific pathogen-free (SPF) conditions at the Centre for Comparative Medicine and Bioimage (CMCIB) animal facility at IGTP in Badalona, Spain. Mice were randomly assigned to cages according to a combination of sex (female/male) and treatment group (Mock/Immunized), with a maximum of 5 animals per cage (Supplementary Fig. 1) and allowed to acclimate for one week before the initial treatment.

### Pre-intervention gut microbial homogenization

To reduce potential baseline differences in the microbiota composition, the mice gut microbiota was homogenized by antibiotic conditioning followed by mouse-to-mouse FMT (1 week after arrival and 2 weeks prior to vaccination). The antibiotic treatment consisted of a combination of ampicillin, amikacin, metronidazole and vancomycin (10 mg/ml each antibiotic), administered via oral gavage (200  $\mu$ l/animal) for 5 days prior to FMT. Mixed stools from five male and five female donor mice (cages MF1 and MM1, Supplementary Fig. 1) were used for FMT in all animals in the study. Briefly, feces from donors were collected, pooled, aliquoted (350 mg vials) and preserved at  $-80^{\circ}\text{C}$  until use. On the day of the fecal transfer, thawed feces were resuspended in sterile physiological saline serum (2.3 ml per vial), homogenized, centrifuged ( $500 \times g$ , 1 min) and supernatant administered by oral gavage (100  $\mu$ l/animal). Bacterial load in FMT was measured using the LIVE/DEAD<sup>®</sup> BacLight<sup>™</sup> Bacterial Viability and Counting Kit (Invitrogen, Carlsbad, MA, USA).

## Immunization strategy

Animals were vaccinated with the HIV T-cell immunogen (HTI), a synthetic protein designed as the fusion of different HIV-1 protein fragments associated with T-cell control of HIV infection<sup>20</sup>. Briefly, the HTI sequence encodes for a 529 amino acid immunogen, designed as the concatenation of 16 clade B consensus HIV Gag, Pol, Vif and Nef protein fragments, which were preferentially targeted by people showing natural control of HIV infection, linked by alanine triplets. The amino acid sequence was back-translated into nucleotides, codon usage optimized for expression in human and the resulting open reading frame (ORF) synthesized to be inserted in different vectors<sup>22</sup>. Specifically, it was inserted into a plasmid DNA under the control of a CMV promoter (DNA.HTI, D) and into two viral vectors: Chimpanzee Adenovirus Ox1 (ChAdOx1.HTI, C) and Modified Vaccinia Ankara (MVA.HTI, M)<sup>22</sup>. HTI vaccine immunogenicity has been previously tested in C57BL/6 mouse model and non-human primates<sup>22</sup> as well as in humans<sup>23</sup>. In this study, twenty mice (10 females and 10 males) were immunized intramuscularly (caudal thigh muscle) with a heterologous prime-boost regime consisting of three different vaccine vectors expressing HTI: (i) three DNA.HTI primes (100 µg/animal), (ii) one boost with ChAd.HTI ( $1 \times 10^9$  VP/animal), and (iii) a second boost with MVA.HTI ( $1 \times 10^6$  pfu/animal). DNA.HTI vaccinations were administered at weeks 0, 3, and 6, followed by ChAd.HTI and MVA.HTI, separated by a 6-week interval (weeks 9 and 15, respectively) (Fig. 1 and Supplementary Fig. 1). Mice in the mock group ( $n=20$ , 10 females and 10 males) were vaccinated with PBS as a control group, following the same immunization schedule.

## Sample collection and processing

Microbiota data were generated in two batches (samples extracted and sequenced in 2019 and 2020), as illustrated in Supplementary Figs. 1 and 2. The first sequencing batch included pooled fecal samples longitudinally collected from cages, whereas the second batch included longitudinal pools of feces from cages and individual fecal samples obtained from different sections of the intestinal tract at the last time point of the study. Longitudinal fecal samples were collected (one pool per cage,  $n=5$ ) at animal arrival (week-3), following antibiotic conditioning prior to FMT (week-2) and prior each vaccination (weeks 0, 3, 6, 9 and 15). Donor pool fecal sample (week-1) was also collected and sequenced in batch 1. Three weeks after the last immunization (week 18), mice were euthanized and luminal contents from three intestinal sections (small, caecum and large intestine), whole blood and spleen were harvested. Serum was separated from the whole blood by centrifugation ( $10,000 \times g$ , 5 min) in Serum Gel S/1.1 tubes (Sarstedt) and frozen at  $-80^\circ\text{C}$  until use. Splenocytes were isolated by mechanical disruption and pressed through a cell strainer (Falcon) using a 5 ml-syringe rubber plunger. Following red blood cell lysis, splenocytes were washed, resuspended in R10 (RPMI 1640 supplemented with 10% fetal bovine serum, 2 mM L-glutamine, 100 U/ml penicillin and 100 µg/ml streptomycin) and cryopreserved in liquid  $\text{N}_2$  until use.

## DNA extraction and 16S rRNA sequencing

Genomic DNA from fecal samples and intestinal content was extracted using the QIAamp DNA Stool Kit, according to the manufacturer's instructions, and stored at  $-80^\circ\text{C}$  until sequencing. Amplification of the V3–V4 hypervariable region of the 16S rRNA gene was performed using universal primers flanked by standard forward and reverse adapters (16S\_F 5'-TCG TCG TCG GCA GCG TCA GAT GTG TAT AAG AGA CAG CCT ACG GGN GGC WGC AG-3'; 16S\_R 5'-GTC TCG TGG GCT CGG AGA TGT GTA TAA GAG ACA GGA CTA CHV GGG TAT CTA ATC C-3') described in the Illumina MiSeq rRNA Amplicon Sequencing protocol (San Diego,

CA, USA). PCR were performed in 25 µL reaction volume, containing 2.5 µL of DNA template, 12.5 µL of KAPA HiFi HotStart Ready Mix (KAPA HiFi HotStart DNA Polymerase, buffer,  $\text{MgCl}_2$ , and dNTPs, KAPA Biosystems Inc., Wilmington, MA, USA) and 5 µL of each primer at 1 µM. Thermocycling conditions were as follows: initial denaturation step at  $95^\circ\text{C}$  for 3 min, followed by 30 cycles of denaturation at  $95^\circ\text{C}$  for 30 s, annealing at  $55^\circ\text{C}$  for 30 s, extension at  $72^\circ\text{C}$  for 30 s and a final extension step at  $72^\circ\text{C}$  for 10 min. Once the expected amplicon size was confirmed on a 1.0% agarose gel electrophoresis (~460 base pairs), PCR products were stored at  $-30^\circ\text{C}$  until sequencing library preparation. Negative extraction and PCR controls (blank controls using DNA-free water as the template) were loaded to assess for potential contamination and processed in the same conditions as any other sample. Amplified DNA templates were cleaned-up with AMPure XP reagent (Beckman Coulter Life Sciences, Indianapolis, USA) for non-DNA molecules and Illumina sequencing adapters and dual indices were attached using Nextera XT index Kit (Illumina Inc.), followed by a corresponding PCR amplification program as described in MiSeq 16S rRNA Amplicon Sequencing protocol (Illumina Inc., San Diego, CA, USA). After the second round of clean-up, amplicon libraries were quantified using a Quant-iT<sup>TM</sup> PicoGreen<sup>®</sup> dsDNA Assay Kit (Invitrogen, Carlsbad, MA, USA) and diluted in equimolar concentrations (4 nM) for further pooling. Pooled libraries were sequenced on an Illumina MiSeq<sup>TM</sup> platform (Illumina Inc., San Diego, CA, USA) at the genomics core facility in Germans Trias i Pujol research campus (Badalona, Spain) using a paired-end 300 base-length protocol.

## Microbiome data analysis

The quality of raw sequencing data was estimated using FastQC<sup>51</sup> and the analysis of 16S rRNA sequences performed using the DADA2 pipeline (v1.10.1)<sup>52</sup>. The pipeline was executed according to default parameters using  $\text{maxEE}=4.10$  in the filtering step. After chimeric reads removal, unique amplicon sequence variants (ASV) were assigned a taxonomy and aligned to the SILVA rRNA gene database<sup>53</sup>. Downstream analyses were conducted in the R environment (v3.5.2)<sup>54</sup> using multiple packages, including *phyloseq* (v1.26.1)<sup>55</sup>, *vegan* (v2.5-5)<sup>56</sup>, *ade4* (v1.7-13)<sup>57</sup> and *ggplot2* (v3.2.0)<sup>58</sup>. ASV counts were normalized and transformed to relative abundance using the phyloseq function *transform\_sample\_counts* ( $100 \times (x/\text{sum}(x))$ ). Alpha diversity (Shannon entropy index) was evaluated using the *estimate\_richness* on rarefied ASV counts. Beta diversity was calculated based on Bray–Curtis distances (normalized data) and distance matrix used to perform an ordination principal coordinate analysis (PCoA).

## Mouse IFN $\gamma$ ELISPOT assay

ELISPOT assays were performed using the mouse IFN $\gamma$  ELISPOT kit (ALP) (Mabtech AB, Stockholm, SE), following the manufacturer's instructions with minor modifications. Briefly, splenocytes were thawed, washed, counted (NucleoCounter<sup>®</sup> NC-3000, Chemometec), cell density adjusted with R10 at  $4 \times 10^5$  cells/well and plated in 96-well polyvinylidene plates (Millipore Corp., Bedford, MA), previously coated with IFN $\gamma$  capture antibody (clone AN-18). Cells were stimulated with 17 HTI-specific peptide pools (14 µg/ml final concentration for each peptide) for 16 h at  $37^\circ\text{C}$  in 5%  $\text{CO}_2$ . A set of 147 overlapping peptides (OLP) of 15 amino acids in length, overlapping by 11 amino acids and covering the entire HTI sequence, were designed using the PeptGen algorithm (Los Alamos HIV database) and synthesized (Synpeptide). To assess responses to HTI, OLP were assembled into 17 separated peptide pools consisting of 7 pools for Gag (8–11 peptides/pool), 7 for Pol (11 or 5 peptides/pool), 2 for Vif (8 and 6 peptides/pool) and 1 for Nef (2 peptides/pool). Concanavalin A (Sigma-Aldrich Corp., Saint Louis, MO), at 5 µg/ml, was used as a positive control and R10 in triplicate as a negative control. After stimulation, spot-forming

cells (SFC) were revealed by adding a biotinylated IFN $\gamma$  detection antibody (clone R4-6A2), streptavidin conjugated with alkaline phosphatase (AP) and AP Conjugate Substrate Kit (Bio-Rad Laboratories, Inc., Irvine, CA). SFC per well were counted using an automated ELISPOT reader system (CTL Analyzers LLC, Cleveland, OH) together with the ImmunoSpot software and the magnitude of responses expressed as SFC per 10<sup>6</sup> splenocytes. Threshold for positive responses was defined as responses that were at least 50 SFC/10<sup>6</sup> spleen cells, the mean SFC/10<sup>6</sup> spleen cells in negative control wells plus 3 standard deviations of the negative control wells, or three times the mean of negative control wells, whichever was higher. Results were given as total magnitude (accumulated response to all the pools; SFC/10<sup>6</sup> PBMCs) and breadth (number of positive pools).

### Luminex assay

Concentrations of CD40 ligand (CD154), GM-CSF, IFN  $\gamma$ , IL-1 $\beta$ , IL-2, IL-4, IL-5, IL-6, IL-10, IL-12 (p70), IL-13, IL-15, IL-17A, IL-17E/IL-25, IL-21, IL-22, IL-23, IL-27, IL-31, IL-33, TNF $\alpha$ , TNF $\beta$  at the end of the study (week 21 wpi) were simultaneously measured in mice sera, in a single batch. Briefly, serum samples were thawed, vortexed and centrifuged at 10000 xg for 10 min before collecting 25  $\mu$ l of serum for further testing. The serum concentration of the 22 cytokines was measured simultaneously using sample duplicates in a customized mouse Th17 magnetic bead panel kit (Milliplex) and a Luminex<sup>®</sup> 200 (Luminex Corp) reader, following manufacturer's instructions.

### Statistical analysis

Differences in alpha diversity and taxa abundance between experimental groups were assessed using the Wilcoxon signed-rank and Kruskal-Wallis test (two sided). For beta diversity, statistical significance was assessed using the pairwise permutational multivariate analysis of variance (PERMANOVA, *adonis*) test. The linear discriminant analysis effect size (LEfSe)<sup>59</sup> was performed to identify discriminant bacterial signatures between Mock and Immunized groups ( $\alpha = 0.05$  and LDA score > 2.0). Associations between cytokines, immune response and bacteria were computed based on Spearman correlation coefficients in combination with Benjamini-Hochberg multiple testing correction using the *rcorr* function within the R/hmisc package. Statistical analyses were performed in the R environment and two-tailed 5% level of significance ( $p$ -value  $\leq 0.05$ ) was considered significant, unless otherwise stated.

### Reporting summary

Further information on research design is available in the Nature Research Reporting Summary linked to this article.

### DATA AVAILABILITY

The raw 16 S rRNA sequencing reads used in this study have been deposited at the Sequence Read Archive (SRA) repository (Bioproject No. PRJEB52963).

### CODE AVAILABILITY

R analysis scripts and data associated with this paper are available at <https://doi.org/10.5281/zenodo.7017193>.

Received: 25 August 2022; Accepted: 12 December 2022;

Published online: 30 December 2022

### REFERENCES

- Zheng, D., Liwinski, T. & Elinav, E. Interaction between microbiota and immunity in health and disease. *Cell Res.* **30**, 492–506 (2020).
- Wojcicki, L., Tan, K. S. W. & Gascoigne, N. R. J. Taming the sentinels: microbiome-derived metabolites and polarization of t cells. *Int. J. Mol. Sci.* **21**, 1–17 (2020).
- Atarashi, K. et al. Induction of colonic regulatory T cells by indigenous Clostridium species. *Science* (1979) **331**, 337–341 (2011).
- Ivanov, I. I. et al. Induction of intestinal Th17 cells by segmented filamentous bacteria. *Cell* **139**, 485–498 (2009).
- Cheng, H., Guan, X., Chen, D. & Ma, W. The th17/treg cell balance: a gut microbiota-modulated story. *Microorganisms* **7**, 583 (2019).
- Gill, N. & Finlay, B. B. The gut microbiota: challenging immunology. *Nat. Rev. Immunol.* **11**, 636–637 (2011).
- Lynn, D. J., Benson, S. C., Lynn, M. A. & Pulendran, B. Modulation of immune responses to vaccination by the microbiota: implications and potential mechanisms. *Nat. Rev. Immunol.* **22**, 33–46 (2021).
- de Jong, S. E., Olin, A. & Pulendran, B. The impact of the microbiome on immunity to vaccination in humans. *Cell Host Microbe* **28**, 169–179 (2020).
- Harris, V. et al. Rotavirus vaccine response correlates with the infant gut microbiota composition in Pakistan. *Gut Microbes* **9**, 93–101 (2018).
- Hagan, T. et al. Antibiotics-driven gut microbiome perturbation Alters immunity to vaccines in humans. *Cell* **178**, 1313–1328.e13 (2019).
- Siegrist, C.-A. Vaccine immunology. *Vaccines* <https://doi.org/10.1016/b978-1-4160-3611-1.50006-4> (2008).
- Cox, R. J. & Brokstad, K. A. Not just antibodies: B cells and T cells mediate immunity to COVID-19. *Nat. Rev. Immunol.* **20**, 581–582 (2020).
- Lynn, M. A. et al. Early-life antibiotic-driven dysbiosis leads to dysregulated vaccine immune responses in mice. *Cell Host Microbe* **23**, 653–660.e5 (2018).
- Pastor-Ibáñez, R. et al. Impact of transcriptome and gut microbiome on the response of hiv-1 infected individuals to a dendritic cell-based hiv therapeutic vaccine. *Vaccines (Basel)* **9**, 694 (2021).
- Borgognone, A. et al. Gut microbiome signatures linked to HIV-1 reservoir size and viremia control. *Microbiome* **10**, 1–15 (2022).
- Eloe-Fadrosch, E. A. et al. Impact of oral typhoid vaccination on the human gut microbiota and correlations with S. Typhi-specific immunological responses. *PLoS One* **8**, e62026 (2013).
- Elizaldi, S. R. et al. Rectal microbiome composition correlates with humoral immunity to HIV-1 in vaccinated Rhesus Macaques. *mSphere* **4**, e00824–e00819 (2019).
- Ng, S. C. et al. Gut microbiota composition is associated with SARS-CoV-2 vaccine immunogenicity and adverse events. *Gut* **71**, 1106–1116 (2022).
- Mothe, B. et al. Definition of the viral targets of protective HIV-1-specific T cell responses. *J. Transl. Med.* **9**, 208 (2011).
- Mothe, B. et al. Ctl responses of high functional avidity and broad variant cross-reactivity are associated with hiv control. *PLoS One* **7**, e29717 (2012).
- Saubi, N. et al. Priming with recombinant BCG expressing HTI enhances the magnitude and breadth of the T-cell immune responses elicited by MVA.HTI in BALB/c mice. *Vaccines (Basel)* **8**, 678 (2020).
- Mothe, B. et al. A human immune data-informed vaccine concept elicits strong and broad T-cell specificities associated with HIV-1 control in mice and macaques. *J. Transl. Med.* **13**, 60 (2015).
- Bailón, L. et al. Safety, immunogenicity and effect on viral rebound of HTI vaccines in early treated HIV-1 infection: a randomized, placebo-controlled phase 1 trial. *Nat. Med.* <https://doi.org/10.1038/s41591-022-02060-2> (2022).
- Wu, M. et al. The differences between luminal microbiota and mucosal microbiota in mice. *J. Microbiol Biotechnol.* **30**, 287–295 (2020).
- Blander, J. M., Longman, R. S., Iliev, I. D., Sonnenberg, G. F. & Artis, D. Regulation of inflammation by microbiota interactions with the host. *Nat. Immunol.* **18**, 851–860 (2017).
- Schuijt, T. J., van der Poll, T., de Vos, W. M. & Wiersinga, W. J. The intestinal microbiota and host immune interactions in the critically ill. *Trends Microbiol.* **21**, 221–229 (2013).
- Pereira, F. C. & Berry, D. Microbial nutrient niches in the gut. *Environ. Microbiol* **19**, 1366–1378 (2017).
- Guevarra, R. B. et al. Oral vaccination against lawsonia intracellularis changes the intestinal microbiome in weaned piglets. *Animals* **11**, 2082 (2021).
- Guo, J. et al. Different immunization methods lead to altered gut flora and varied responses to Mycobacterium tuberculosis infection in mice. *J. Infect. Dev. Ctries* **14**, 1170–1177 (2020).
- Tamanai-Shacoori, Z. et al. Roseburia spp.: a marker of health? *Future Microbiol.* **12**, 157–170 (2017).
- Lucas, S., Ghilardi, N., Li, J., Dé, F. & de Sauvage, R. J. IL-27 regulates IL-12 responsiveness of naïve CD4 T cells through Stat1-dependent and-independent mechanisms. *Proc. Natl Acad. Sci USA* **100**, 15047–15052 (2003).
- Dainichi, T., Richards, C. D., Karin, N. & West, N. R. Coordination of immune-stroma crosstalk by IL-6 family cytokines. *Front. Immunol.* **1**, 1093 [www.frontiersin.org](http://www.frontiersin.org) (2019).
- Shohan, M. et al. Interleukin-22 and intestinal homeostasis: protective or destructive? *IUBMB Life* **72**, 1585–1602 (2020).
- Fu, X., Liu, Z., Zhu, C., Mou, H. & Kong, Q. Nondigestible carbohydrates, butyrate, and butyrate-producing bacteria. *Crit. Rev. Food Sci. Nutr.* **59**, S130–S152 (2019).



35. Cheng, H., Guan, X., Chen, D. & Ma, W. The Th17/Treg cell balance: a gut microbiota-modulated story. *Microorganisms* <https://doi.org/10.3390/microorganisms7120583> (2019).
36. Awate, S., Sibiak, L. A., Mutwiri, G., Fournel, S. & Massari, P. Mechanisms of action of adjuvants. *Front. Immunol.* <https://doi.org/10.3389/fimmu.2013.00114> (2013).
37. Pulendran, B., S. Arunachalam, P. & O'Hagan, D. T. Emerging concepts in the science of vaccine adjuvants. *Nat. Rev. Drug Discov.* **20**, 454–475 (2021).
38. Ansar, W. & Ghosh, S. *Infl Ammation and Infl Ammatory Diseases, Markers, and Mediators: Role of CRP in Some Infl amatory Diseases Abstract.* [https://doi.org/10.1007/978-81-322-2680-2\\_4](https://doi.org/10.1007/978-81-322-2680-2_4) (2016).
39. Mazzoni, A. & Segal, D. M. Controlling the toll road to dendritic cell polarization. *J. Leukoc. Biol.* **75**, 721–730 (2004).
40. David, L. A. et al. Diet rapidly and reproducibly alters the human gut microbiome. *Nat.* **2013** 505:7484 **505**, 559–563 (2013).
41. di Sabatino, A. et al. Oral butyrate for mildly to moderately active Crohn's disease. *Aliment Pharm. Ther.* **22**, 789–794 (2005).
42. Guo, Y., Kitamoto, S. & Kamada, N. Microbial adaptation to the healthy and inflamed gut environments. <https://doi.org/10.1080/19490976.2020.1857505> (2020).
43. Omenetti, S. & Pizarro, T. T. The Treg/Th17 axis: A dynamic balance regulated by the gut microbiome. *Front. Immunol.* **6**, 639 (2015).
44. Lin, Y., Slight, S. R. & Khader, S. A. Th17 cytokines and vaccine-induced immunity. *Semin. Immunopathol.* **32**, 79–90 (2010).
45. Henke, M. T. et al. *Ruminococcus gnavus*, a member of the human gut microbiome associated with Crohn's disease, produces an inflammatory polysaccharide. *Proc. Natl Acad. Sci. USA* **116**, 12672–12677 (2019).
46. Ashkar, A. A., Mossman, K. L., Coombes, B. K., Gyles, C. L. & Mackenzie, R. FimH adhesin of type 1 fimbriae is a potent inducer of innate antimicrobial responses which requires TLR4 and type 1 interferon signalling. *PLoS Pathog.* **4**, 14430 (2008).
47. Hill, C. et al. Expert consensus document: the international scientific association for probiotics and prebiotics consensus statement on the scope and appropriate use of the term probiotic. *Nat. Rev. Gastroenterol. Hepatol.* **11**, 506–514 (2014).
48. Luu, M. et al. Regulation of the effector function of CD8+ T cells by gut microbiota-derived metabolite butyrate. *Sci. Rep.* <https://doi.org/10.1038/s41598-018-32860-x> (2018).
49. Jenabian, M.-A. et al. Immunosuppressive tryptophan catabolism and gut mucosal dysfunction following early HIV infection. *J. Infect Dis.* <https://doi.org/10.1093/infdis/jiv037> (2015).
50. Tarabichi, Y. et al. The administration of intranasal live attenuated influenza vaccine induces changes in the nasal microbiota and nasal epithelium gene expression profiles. *Microbiome* **3**, 74 (2015).
51. Andrews, S., Krueger, F., Seconds-Pichon, A., Biggins, F. & Wingett, S. FastQC. A quality control tool for high throughput sequence data. *Babraham Bioinformatics. Babraham Inst.* **1**, 1 (2015).
52. Callahan, B. J. et al. DADA2: High-resolution sample inference from Illumina amplicon data. *Nat. Methods* **13**, 581–583 (2016).
53. Quast, C. et al. The SILVA ribosomal RNA gene database project: Improved data processing and web-based tools. *Nucleic Acids Res.* <https://doi.org/10.1093/nar/gks1219> (2013).
54. R Foundation for Statistical Computing. *R: A Language and Environment for Statistical Computing.* <http://www.R-project.org/> (2018).
55. McMurdie, P. J. & Holmes, S. Phyloseq: An R package for reproducible interactive analysis and graphics of microbiome census data. *PLoS One* **8**, e61217 (2013).
56. Oksanen, J. et al. vegan: Community ecology package. R package version 2.5-2. *Cran R.* **1**, 2 (2019).
57. Dray, S. & Dufour, A.-B. The ade4 Package: implementing the duality diagram for ecologists. *J. Stat. Softw.* <https://doi.org/10.18637/jss.v022.i04> (2015).
58. Wickham, H. *Package 'ggplot2': Elegant Graphics for Data Analysis* (Springer-Verlag, 2016).
59. Segata, N. et al. Metagenomic biomarker discovery and explanation. *Genome Biol.* **12**, R60 (2011).

## ACKNOWLEDGEMENTS

The project received funding from the European Union's Horizon 2020 Research and Innovation programme under Grant Agreement No. 847943 (MISTRAL) and was sponsored in part by Grifols.

## AUTHOR CONTRIBUTIONS

M.N.-J., C.B., A.O. and R.P. designed the study and supervised the research. A.B. analyzed the data and wrote the manuscript. A.E.-T. contributed to data interpretation and redaction of the manuscript. A.E.-T., M.C. and A.O. set up the animal experiments and collected samples. A.E.-T., M.C. and M.P. performed fecal DNA extraction, library preparation and sequencing. L.R., T.E. and A.O. performed cytokine profiling and immune response determinations. F.C.-M., M.N.-J. and A.B. contributed to data processing, management, and storage. A.B. and A.E.-T. are co-first authors of the manuscript. A.O. and R.P. are co-corresponding authors of the manuscript. All authors edited drafts critically, revised the manuscript, and approved the final version as submitted.

## COMPETING INTERESTS

The authors declare no competing interests.

## ETHICAL APPROVAL

All experiments involving animals were approved by the Animal Experimentation Ethics Committee of the Germans Trias i Pujol Hospital (IGTP) and the Generalitat de Catalunya (Project number: 10559).

## ADDITIONAL INFORMATION

**Supplementary information** The online version contains supplementary material available at <https://doi.org/10.1038/s41522-022-00368-y>.

**Correspondence** and requests for materials should be addressed to Alex Olvera or Roger Paredes.

**Reprints and permission information** is available at <http://www.nature.com/reprints>

**Publisher's note** Springer Nature remains neutral with regard to jurisdictional claims in published maps and institutional affiliations.



**Open Access** This article is licensed under a Creative Commons Attribution 4.0 International License, which permits use, sharing, adaptation, distribution and reproduction in any medium or format, as long as you give appropriate credit to the original author(s) and the source, provide a link to the Creative Commons license, and indicate if changes were made. The images or other third party material in this article are included in the article's Creative Commons license, unless indicated otherwise in a credit line to the material. If material is not included in the article's Creative Commons license and your intended use is not permitted by statutory regulation or exceeds the permitted use, you will need to obtain permission directly from the copyright holder. To view a copy of this license, visit <http://creativecommons.org/licenses/by/4.0/>.

© The Author(s) 2022